J Mater Sci (2010) 45:871–887
DOI 10.1007/s10853-009-4015-5

Volume and thermal studies for tellurite glasses

R. El-Mallawany · A. Abdel-Kader · M. El-Hawary · N. El-Khoshkhany

Received: 13 May 2009 / Accepted: 31 October 2009 / Published online: 24 November 2009

Abstract Binary tellurite glass systems of the forms $TeO_2(100 - x) - xA_nO_m$ where $A_nO_m = La_2O_3$ or V_2O_5 and $x = 5$, 7.5, 10, 12.5, 15, 17.5, and 20 mol% for La_2O_3 and 10, 20, 25, 30, 35, 40, 45, and 50 mol% for V_2O_5 were prepared. Density and molar volume of each glass were measured and calculated. The compressibility model has been used to find the difference volume V_d due to the exchange of one formula unit between Te and both of La and V in the binary glass system and the mean volume V_A per formula unit in the present binary glass in order to check whether or not it is independent of the percentage of the modifier for a glass series and also different from series to another. Differential scanning calorimetric at different heating rates was used to gain some insight into the thermal stability and calorimetric behavior of the present binary transition metal and rare-earth tellurite glasses. The glass transformation temperature T_g and glass crystallization temperature T_c were recorded at different heating rates to calculate both of the glass transition activation and the glass crystallization activation energies by using different methods.

Introduction

Tellurite glasses exhibit a range of unique properties of potential applications as pressure sensors or as new laser hosts. The physical properties and structure of crystalline solids are understood now, but this is not the case for amorphous materials. The considerable theoretical difficulties experienced for amorphous solids are amplified by the lack of precise experimental information. This study is carried out to fill this gap. The mutual benefits of the proposed cooperative research effort are seen as providing the fundamental base for finding new optical glasses with new applications especially (tellurite-based glass optical fiber) which are of interest of all countries all over the world. The physical properties of tellurite glasses have been collected in and also an introduction to "Telluirte Glasses" lecture has been provided as resource for the entire international glass community available in video streaming format on the IMI website [1].

Previously, the thermal behavior of tellurite glass systems has been studied by using the differential thermal analysis (DTA) to measure the glass transformation temperature T_g, or specific heat capacity C_p in the temperature range starting from room temperature to above the T_g. Structural, vibrational investigations on thermal properties, devitrification, vitrification, calorimetric study, and glass stability of tellurite glasses have been measured [2–9]. The present objective is to measure glass transition temperature T_g, crystallization temperature T_c, and onset of crystallization temperature T_x, and also to calculate glass stability against crystallization S and glass-forming tendency K_g. The above experimental parameters will be interpreted quantitatively according to the structure parameters like average cross-link density n'_c, number of bonds per unit volume n_b and average stretching force constant $\bar{F}$ for every glass composition. Also the calculate glass transition activation energy and the glass crystallization activation energy have been calculated using different methods like Chen's, Monihan's, Kissinger's, and

A. Abdel-Kader—deceased.

R. El-Mallawany (✉) · A. Abdel-Kader · M. El-Hawary · N. El-Khoshkhany
Physics Department, Faculty of Science, Menoufia University, Shebin El-Koom, Egypt
e-mail: relmallawany@hotmail.com

Ozawa's models for the very important tellurite glass systems, e.g., semiconducting tellurite vanadate glass [10, 11] and high non-linear optical properties lanthanide tellurite glasses [12].

Experimental work

Glass preparation, vitreous state, and density measurements

The binary glass system $(100 - x)TeO_2 - (x)A_nO_m$ was prepared by mixing all specified weights of tellurium oxide (TeO_2, 99.99% purity, BDH), A_nO_m = lanthanum oxide (La_2O_3, 99.99% purity, BDH) where $x = 5$, 7.5, 10, 12.5, 15, 17.5, and 20 mol% and vanadium oxide (V_2O_5, 99.99% purity, BDH) where $x = 10$, 20, 25, 30, 35, 40, 45, and 50 mol%. The diffusion process took place through an agate mortar and the mixture was thoroughly ground for 20 min. The powdered mixture was then put into an alumina crucible and heated in a melting furnace. In order to reduce any tendency of volatilization, the mixture was kept at 300 °C for 15 min. The crucible was then kept in the same furnace above 300 °C, the value of these temperature depend upon the composition of each sample and its melting temperature. After reaching the required temperature (850–900 °C), the mixture was left for 20 min. To improve the homogeneity, the melt was stirred from time-to-time with an alumina rod. The melt which had a high viscosity was cast at room temperature in a split mold made from mild steel. The sample was transferred after that to the annealing furnace. After 1 h at 300 °C, the annealing furnace was then switched off and the glass rod was allowed to cool inside it for 24 h. The two glass opposite faces were ground roughly approximated parallel on a lapping machine with 600 grade SiC powder. Opposite faces were finished optically flat and parallel with a high

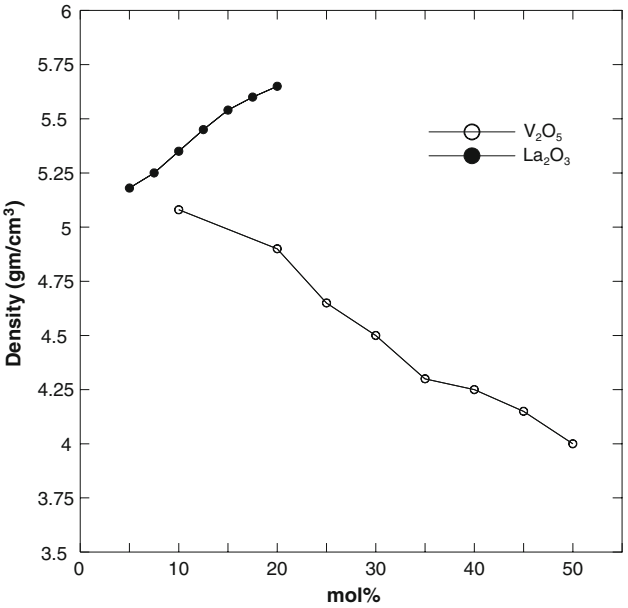

Fig. 1 Variation of density with La_2O_3 content (mol%) for $(TeO_2)_{(100-x)} - (La_2O_3)_x$ glasses and with V_2O_5 content (mol%) for $(TeO_2)_{(100-x)} - (V_2O_5)_x$ glasses

Table 1 Density, molar volume, number of bonds per unit volume, and average force constant of binary tellurite glasses

Glass composition	ρ (gm/cm^3) using Eq. 1	V (cm^3) using Eq. 2	N_b (10^{28} m^{-3}) using Eq. 5	F (N/m) using Eq. 6
TeO_2 glass [13]	5.105	31.26	7.74	
TeO_2 crystal [14]	5.99	26.6		
TeO_2–La_2O_3				
95–5	5.18	32.42	8.07	196.7
92.5–7.5	5.22	32.98	8.25	188.8
90–10	5.32	33.11	8.55	181.8
87.5–12.5	5.42	33.31	8.83	175.6
85–15	5.51	33.5	9.11	170.1
82.5–17.5	5.60	33.68	9.39	165.0
80–20	5.64	34.21	9.58	160.5
TeO_2–V_2O_5				
90–10	5.04	32.11	7.69	234.8
80–20	4.9	33.48	7.55	246.5
75–25	4.64	35.60	7.19	250.9
70–30	4.5	36.95	7.01	254.5
65–35	4.26	39.30	6.67	257.7
60–40	4.24	39.74	6.66	260.4
55–45	4.16	40.78	6.57	262.7
50–50	4.01	42.58	6.36	264.8

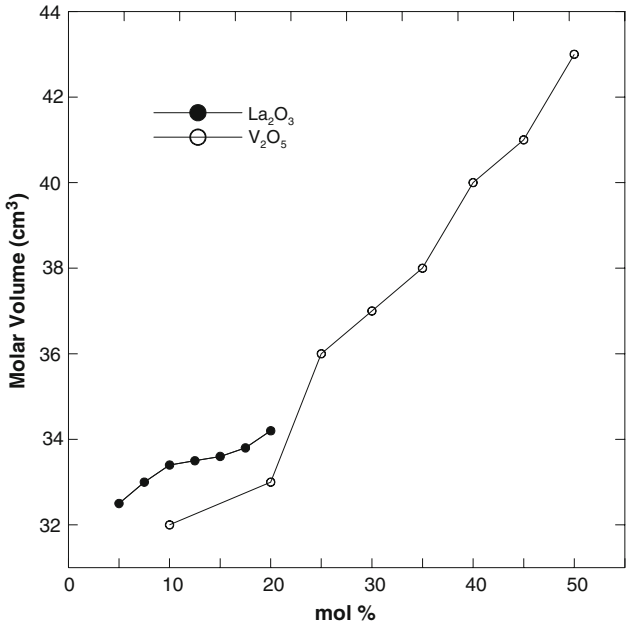

Fig. 2 Variation of molar volume with La_2O_3 content (mol%) for $(TeO_2)_{(100-x)} - (La_2O_3)_x$ glasses and with V_2O_5 content (mol%) For $(TeO_2)_{(100-x)} - (V_2O_5)_x$ glasses

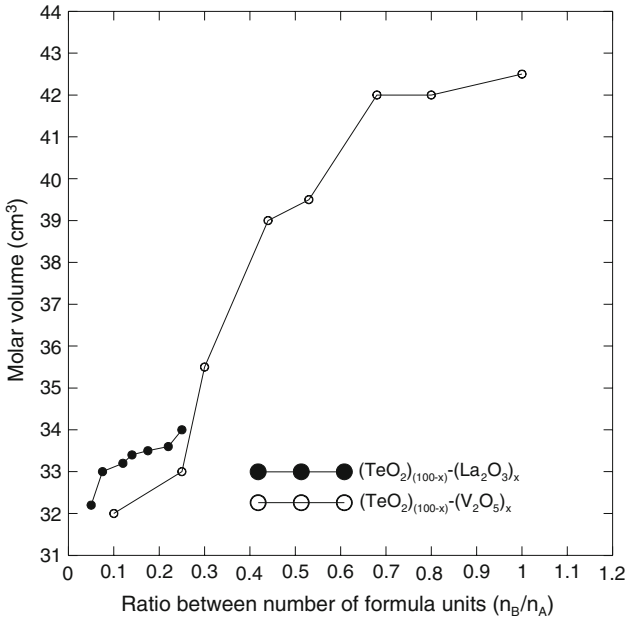

Fig. 3 Variation of the molar volume with the ratio between the number of network formula units (n_B/n_A) for $(TeO_2)_{(100-x)} - (La_2O_3)_x$ glasses and for $(TeO_2)_{(100-x)} - (V_2O_5)_x$ glasses

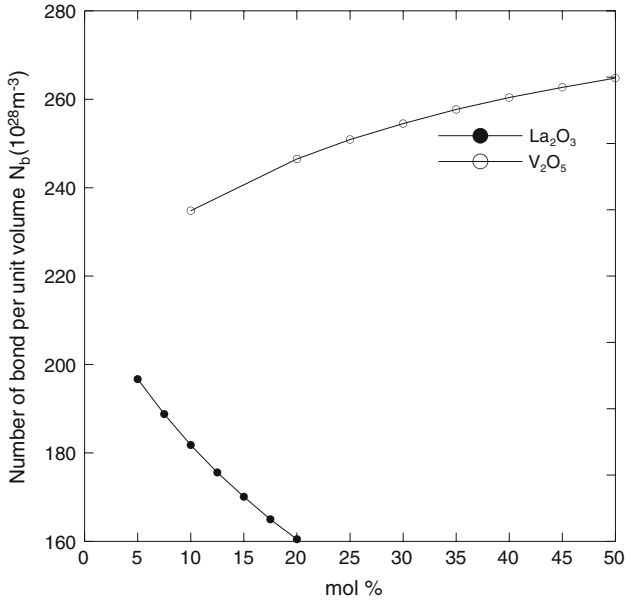

Fig. 4 Variation of N_b (the number of bond per unit volume) with La_2O_3 content (mol%) for $(TeO_2)_{(100-x)} - (La_2O_3)_x$ glasses and with V_2O_5 content (mol%) for $(TeO_2)_{(100-x)} - (V_2O_5)_x$ glasses

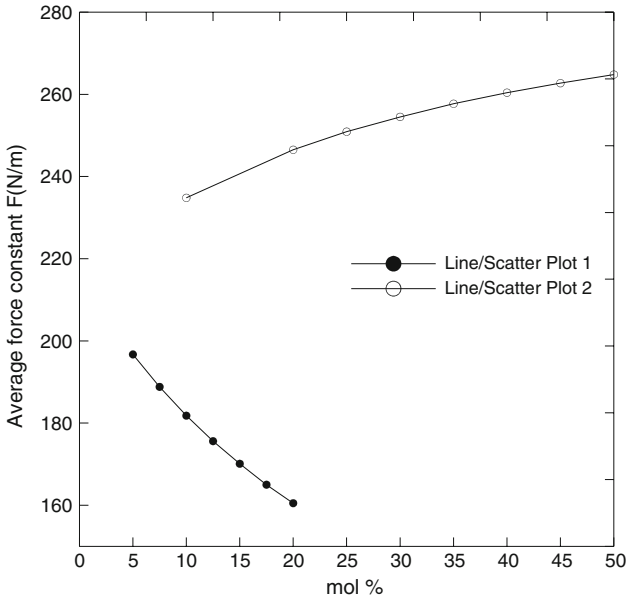

Fig. 5 Variation of the average force constant F with La_2O_3 content (mol%) for $(TeO_2)_{(100-x)} - (La_2O_3)_x$ glasses and with V_2O_5 content (mol%) for $(TeO_2)_{(100-x)} - (V_2O_5)_x$ glasses

mirror-like surface. As both the preparation and annealing furnace had capacities greatly exceeding the volume of the crucible, the temperature gradients in the volume of the crucible, the temperature gradients across the glass at any time during melting and annealing were constant. The glass formed was therefore expected to be homogeneous. Table 1 gives the composition of the glass samples investigated in this study.

The vitreous state of two binary systems was examined by X-ray diffraction using a Shimadzu diffractometer (Model XD-3). The density of the prepared glassy samples was determined at room temperature by a simple Archimedes method, using toluene as an immersion liquid. The

density of each composition was then obtained by using the following relation

$$\rho_g = \frac{W_a \rho_L}{(W_a - W_L)} \quad (1)$$

where ρ_L is the relative density of the liquid toluene (0.864 g/cm^3 at 25 °C), W_a and W_L are the weights of the glass sample in air and in the liquid, respectively. The molar volume V (i.e., the volume occupied by one gram molecule of the glass) was calculated by the following expression:

$$V = \frac{(xM_A + yM_B)}{\rho_g} \quad (2)$$

where the glass composition is represented by x and y and $x + y = 100\%$ and M_A, M_B are the molecular weights of materials A and B forming the glassy network.

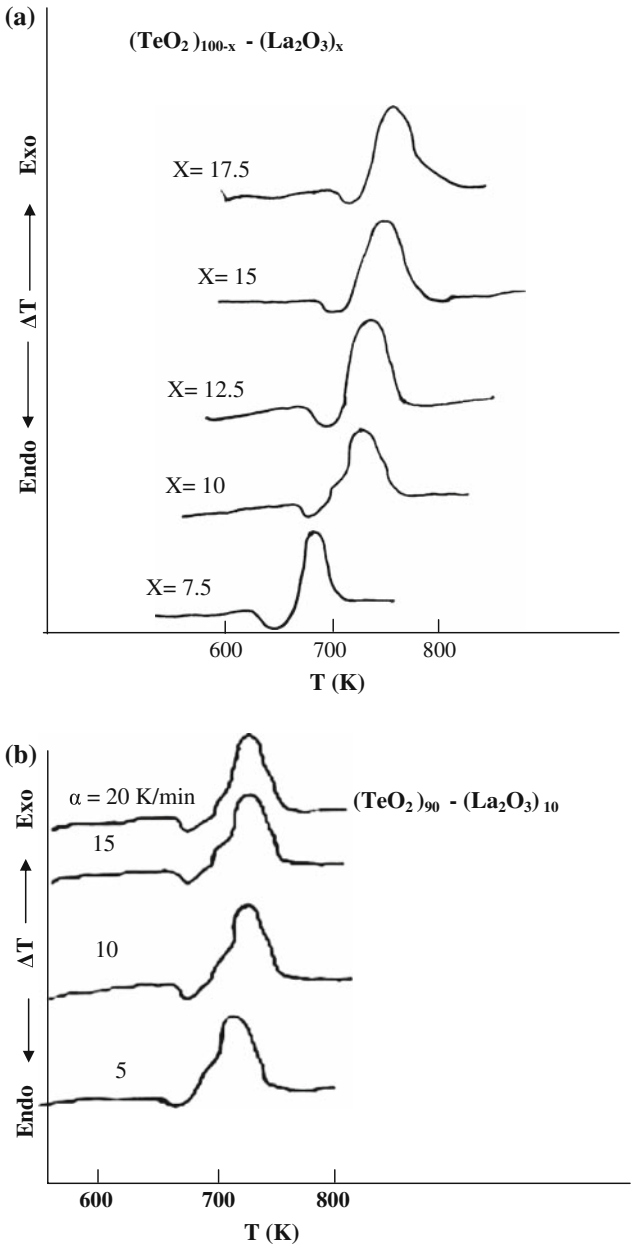

Fig. 6 **a** Typical DSC traces of the prepared binary lanthanum tellurite glasses for different compositions at heating rate 10 K/min. **b** Typical DSC traces of the prepared binary $(TeO_2)_{90} - (La_2O_3)_{10}$ glasses for different heating rates

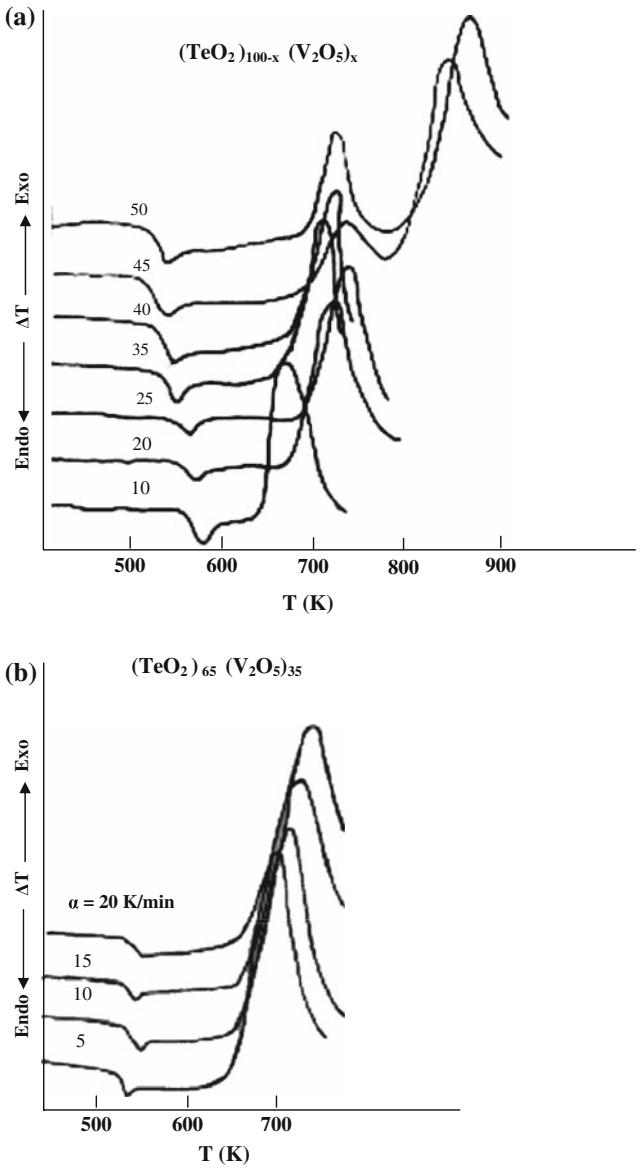

Fig. 7 **a** Typical DSC traces of the prepared binary vanadium tellurite glasses for different compositions at heating rate 10 K/min. **b** Typical DSC traces of the prepared binary $(TeO_2)_{65} - (V_2O_5)_{35}$ glasses for different heating rate

Thermal measurements

The thermal behavior was investigated using differential scanning calorimetric (DSC; Shimadzu 50 DSC). The temperature and energy calibrations of the instrument were performed using the well-known melting temperature and melting enthalpy of high-purity indium metal. The calorimetric sensitivity is 10 μW and the temperature accuracy is ±1.0 K. The crystallization thermogram of the sample was recorded as the temperatures of the samples were increased at a uniform heating rate α at 5, 10, 15, and 20 K/min. Typically, than 50 μW was scanned over a temperature range from room temperature to about 500 K. The melting temperature was determined by using DTA (Shimadzu 30 DTA).

Results and discussion

The X-ray diffraction tests of the prepared glasses in the powder form do not show any peaks, indicating that the structures of the prepared samples are, in generally, amorphous.

Density and molar volume results

The results of the density measurements for the produced glasses are shown in Fig. 1. Table 1 shows the variation of both density and molar volume for all glasses collected for both binary tellurite glass series and pure TeO_2 glass [13]. It is informative to compare the densities of pure TeO_2 crystal and the pure TeO_2 glass [14]; the ratio of this parameter was 1.18. The fact that the density of the glass was smaller than that of the crystal correlates extremely well with the reduced number of TeO_2 units that could be accommodated in the more open structure of the vitreous state. For binary (La_2O_3 and V_2O_5) tellurite glasses, both ρ and V depended on the percentage and type of the modifier used. The results showed that the density increased from 5.18 to 5.64 g/cm^3 with increasing La_2O_3 content (5–20 mol%). The density also decreased from 5.04 to 4.01 g/cm^3 with the increase in V_2O_5 (10–50 mol%).

This change in density accompanying the addition of La_2O_3 or V_2O_5 is due to the change in the atomic mass and atomic volume of constituent elements. The atomic mass of Te, La, and V atoms are 127.6, 138.91, and 50.942, respectively, and their atomic radii are 1.6, 1.87, and 1.34 Å, respectively. This explains the observed increasing

Table 3 The glass transition temperature and the glass transition activation energies of binary tellurite glasses

Glass composition	T_g (K)	E_t (kJ/mol) using Eq. 10	E_t (kJ/mol) using Eq. 11
TeO_2–La_2O_3			
92.5–7.5	624	285.71	296.0
90–10	666	291.67	302.31
87.5–12.5	675	355.06	366.3
85–15	684	390.34	401.8
82.5–17.5	705	392.32	403.9
TeO_2–V_2O_5			
90–10	563	585.58	594.96
80–20	550	571.16	580.32
75–25	538	500.31	509.24
65–35	525	436.12	446.82
60–40	519	351.99	360.65
55–45	512	344.01	352.48
50–50	511	281.25	289.79

Table 2 Thermal properties of the binary tellurite glasses

Glass composition	T_g (K)	T_x (K)	T_c (K)	T_m (K)	$(T_x - T_g)$ (K)	(T_g/T_m)	$(T_c - T_g)$ (K)	$K_g = (T_c - Tg)/(T_m - T_c)$
TeO_2 glass [13]	598	673	713	933	75	0.6	115	0.41
TeO_2–La_2O_3								
92.5–7.5	624	661	676	923	37	0.68	52	0.21
90–10	666	687	726	928	21	0.72	60	0.3
87.5–12.5	675	707	735	921	32	0.73	60	0.32
85–15	684	708	747	944	24	0.72	63	0.32
82.5–17.5	705	730	755	953	25	0.74	50	0.25
TeO_2–V_2O_5								
90–10	563	646	664	993	83	0.57	101	0.31
80–20	550	664	721	1160	114	0.47	171	0.39
75–25	538	676	732	1166	138	0.46	194	0.45
65–35	525	652	705	1170	127	0.45	180	0.39
60–40	519	677	714	1173	158	0.44	195	0.42
55–45	512	685	724	1178	173	0.43	212	0.47
50–50	511	686	714	1180	175	0.43	203	0.44

and decreasing with increasing La_2O_3 or V_2O_5 content. The molar volume V was calculated from Eq. 2. The change of molar volume versus mol% concentration of La_2O_3 and V_2O_5 is shown in Fig. 2. The calculated molar volume of the pure TeO_2 crystal and TeO_2 glass was 26.6 and 31.29 cm^3, respectively [13]. This means that the ratio $V_{glass}/V_{crystal}$ is 1.18, i.e., the change is only 18% from crystalline solid to be non-crystalline solid. Hence, the fact that molar volume of the glass is greater than that of the crystal which correlates extremely well with longer number of TeO_2 units that can be accommodated in the more open structure of the vitreous state. For the first series of binary TeO_2–La_2O_3, the molar volume increased from 32.42 to 34.21 cm^3. Also for the second series TeO_2–V_2O_5 glass, the molar volume increased from 32.11 to 42.58 cm^3 as shown in Fig. 2. The molar volume of binary vanadium tellurite glasses or binary lanthanum tellurite glasses would be higher than pure TeO_2 glass, as shown in Table 1.

The structural interpretation will be based on the simple model of compressibility by Mukherjee et al. [15] of binary glass A_xB_{1-y} containing n_A formula units of type A and n_B formula units of type B with the percentage $x = n_A/(n_B + n_A)$ has stated a relation to find the volume. The volume of the binary glass containing n_A (Avogadro's number) formula units of type A and n_B formula unit of type B can be easily determined from the density measurements using the following relation

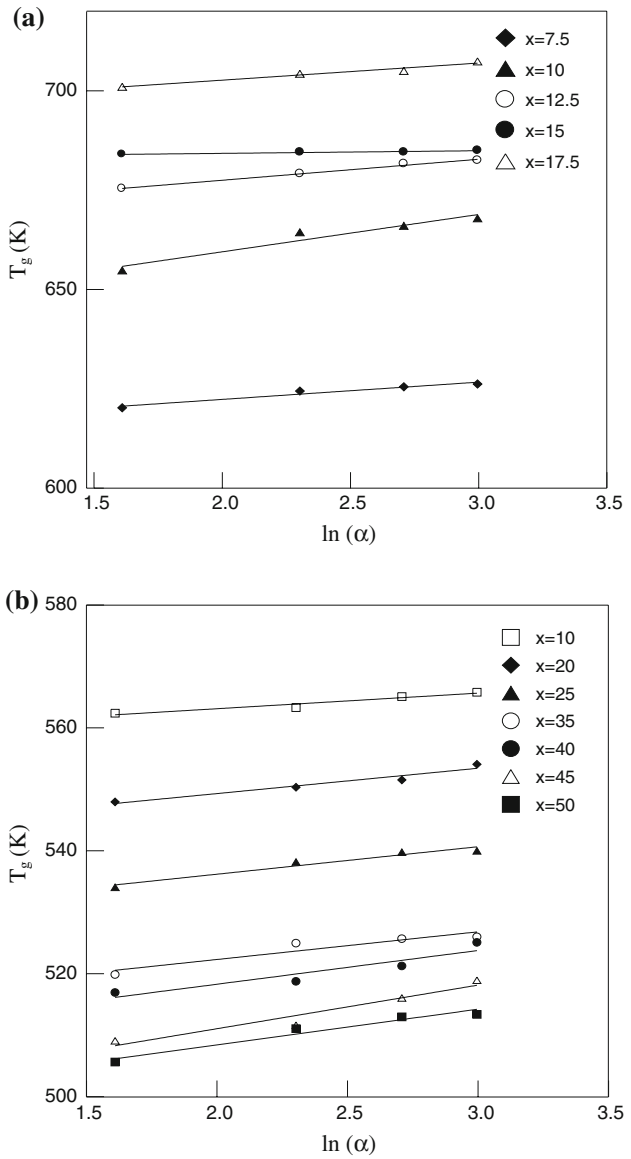

Fig. 8 Variation of T_g versus ln(α) for **a** $(TeO_2)_{(100-x)} - (La_2O_3)_x$ glasses and **b** $(TeO_2)_{(100-x)} - (V_2O_5)_x$ glasses

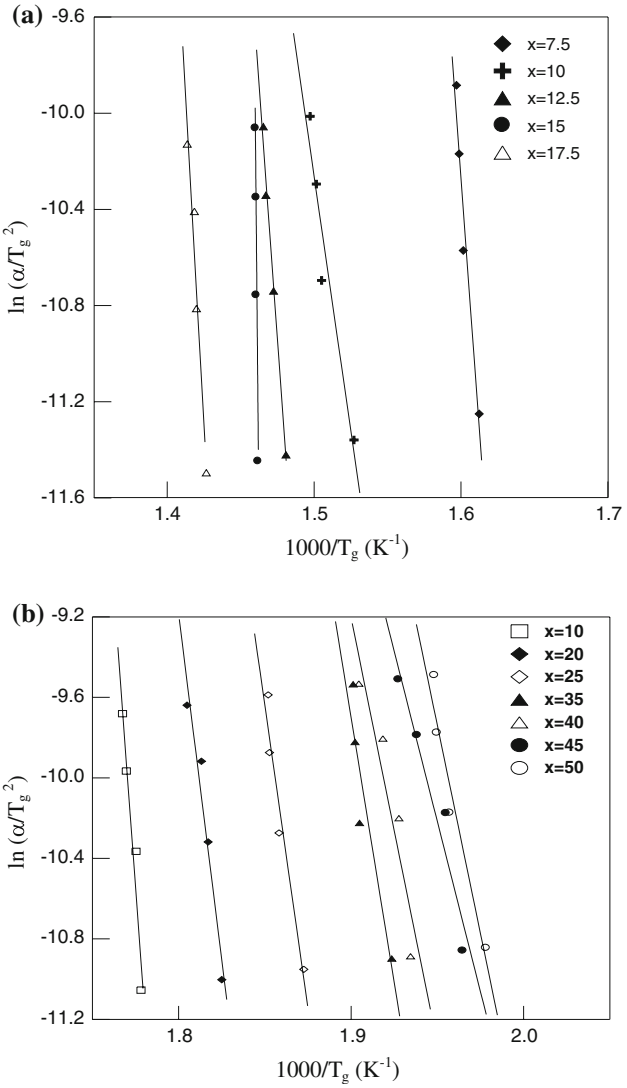

Fig. 9 Variation of $\ln(\alpha/T_g^2)$ versus $(1000/T_g)$ for **a** $(TeO_2)_{(100-x)} - (La_2O_3)_x$ glasses and **b** $(TeO_2)_{(100-x)} - (V_2O_5)_x$ glasses

$$V = \frac{[M_A + (n_B/n_A)M_B]}{\rho} \quad (3)$$

where ρ is the density of the binary glass A_XB_{1-X}, and M_A and M_B are the molecular weights of the formula units A and B, respectively, and x is the percentage. The model supposed that the composition of binary glass AB changes from n_A and n_B formula units of types A and B, respectively, to $n_A - 1$ and $n_B + 1$ corresponding formula units. While the total number of formula units of A and B taken together remains unchanged, the volume of the vitreous system changes by an amount which called the difference volume V_d due to the exchange of one formula unit between A and B in the binary glass system. The compressibility model assumed that the difference volume V_d and the mean volume V_A per formula unit of A in the binary glass A_XB_{1-X} independent of the percentage of the modifier for a glass series and different from series to another. Also, the model restricted that the binary glass series has the same structure and no phase changes. This implies that the volume V of the binary system A_XB_{1-X} containing n_A (Avogadro's number) formula units of A and n_B formula units of B has been written as:

$$V = n_AV_A + n_B(V_d + V_A) = V_0 + (n_B/n_A)(n_AV_d + V_0) \quad (4)$$

where $V_0 = n_AV_A$ represents the molar volume of the vitreous system consisting of n_A formula units of type A only with the mean volume equal to V_A per formula unit and (n_B/n_A) is the composition ratio. Although we do envisage the molecular units in the glass network, where A stands for the glass former TeO_2 and B stands for the modifier, i.e., any one of La_2O_3 or V_2O_5. Equation 4 clearly indicates that the plot of V against the composition ratio (n_B/n_A) follows a straight line from which the intersect with Y-axis gives V_0 and the slope gives $(n_AV_d + V_0)$. From Fig. 3, it was found that, for the two binary tellurite glasses studied in this study, the value of V_0 is 32.1717 cm^3 for the line of TeO_2–La_2O_3 and 31.3645 cm^3 for the line TeO_2–V_2O_5, respectively. The calculated values of the volume obtained from the sample model agreed with the experimental values of the pure TeO_2 [13]. From the slope of both lines in Fig. 3 and by using Eq. 4, the values of the quantity (n_AV_d) are −24.373 and −19.396 cm^3 for the two binary glass series, respectively. These values are negative while binary V_2O_5–P_2O_3 glasses have the value of +9.538 cm^3 as stated by Mukherjee et al. [15]. This change in molar volume was due to the change in the structure caused by the change on interatomic spacing, which could be attributed to the change in the number of bonds per unit volume of the glassy network and change of the stretching force constant of the bonds inside the glassy network. El-Mallawany [7] has used the Mukherjee model and calculated V_0 of pure TeO_2 and also for the binary TeO_2–MoO_3 glasses. The calculated value of V_A for pure TeO_2 is 10.41 cm^3, and for 20 mol% TeO_2–MoO_3, V_A = 9.76 and 9.4 cm^3, 50 mol%, whereas for 20 mol% TeO_2–V_2O_5, V_A = 9.3 and 8.54 cm^3, 50 mol%.

Now for more quantitative analysis, we calculate N_b, the number of bonds per unit volume of the glass given by

$$N_b = \sum n_f(N_f) = \sum n_f\left\{\frac{N_A\rho}{M_g}\right\} \quad (5)$$

where n_f is the number of network bonds per unit glass formula and equal to the coordination number of each cation times the number of cations in the glass formula unit, N_f is the number of formula units per volume, N_A is Avogadro's number ρ is the glass density and M_g is the molecular weight of the glass. Figure 4 shows a plot of number of bonds per unit volume versus mol% concentration of La_2O_3 and V_2O_5, respectively. After

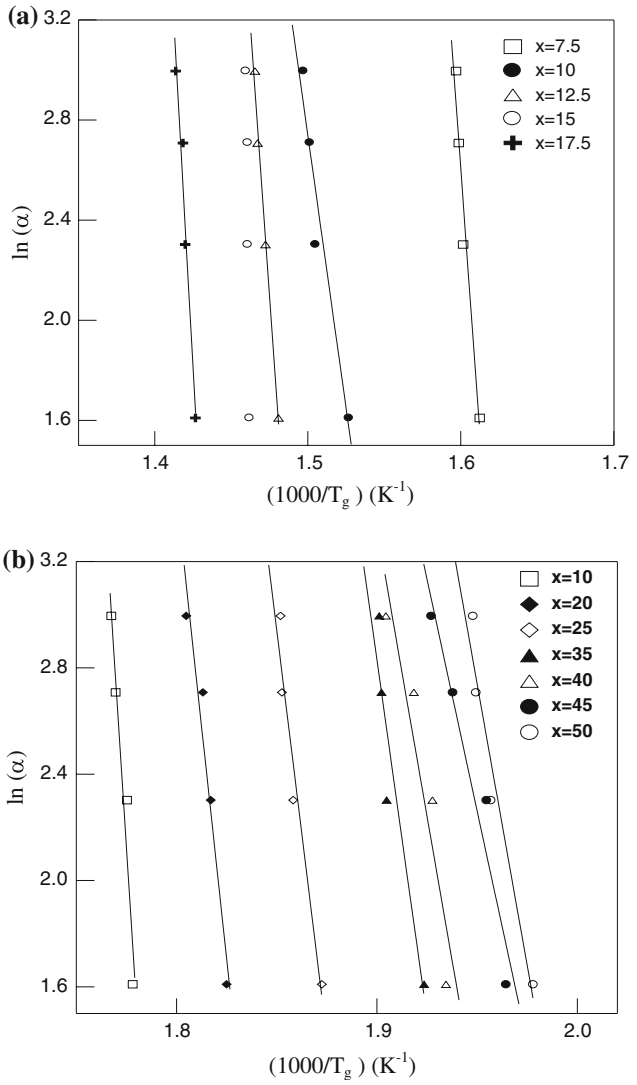

Fig. 10 Variation of ln(α) versus (1000/T_g) for **a** $(TeO_2)_{(100-x)} - (La_2O_3)_x$ glasses and **b** $(TeO_2)_{(100-x)} - (V_2O_5)_x$ glasses

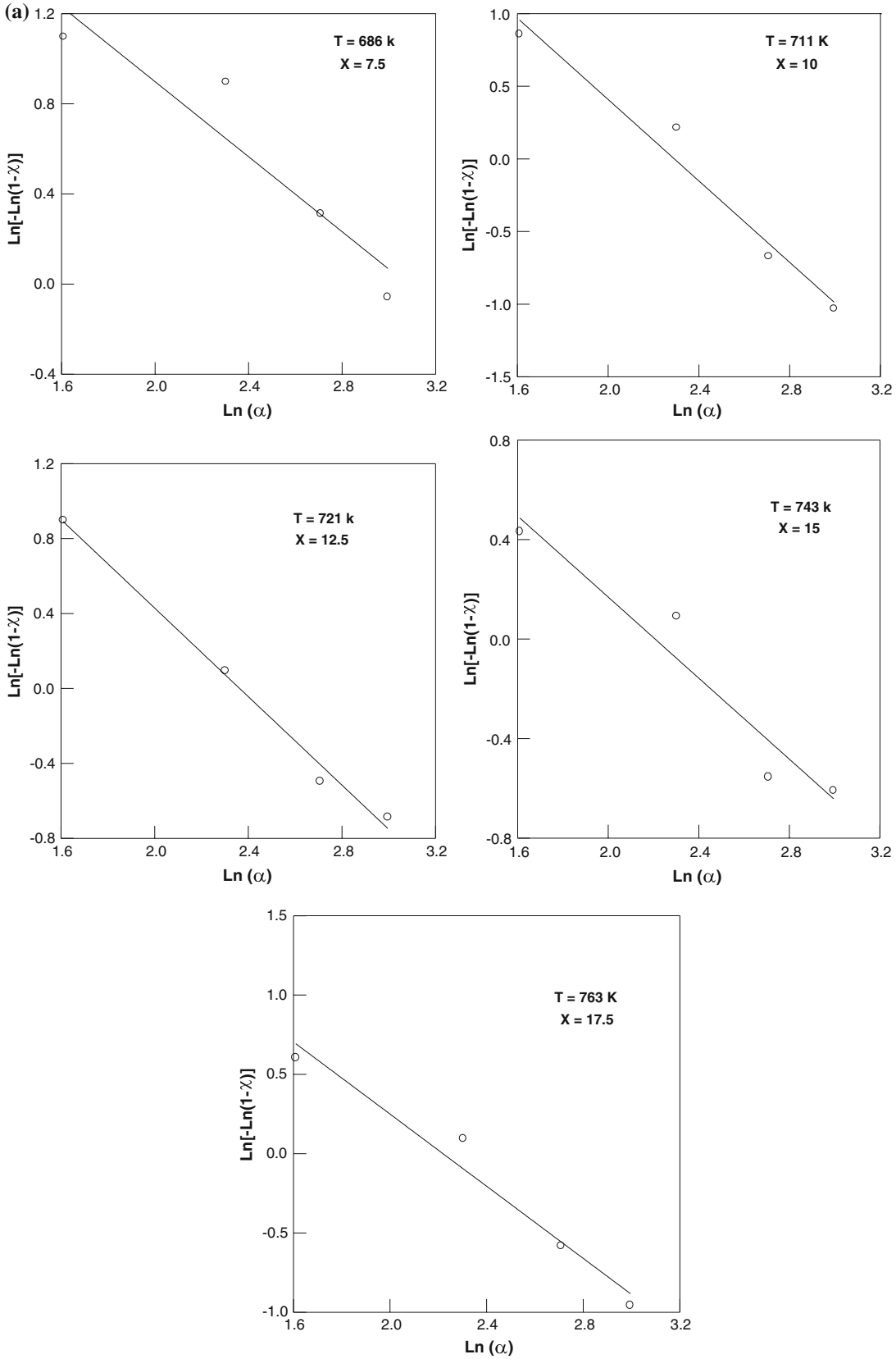

Fig. 11 Variation of $\ln(-\ln(1-\chi))$ versus $\ln(\alpha)$ for **a** $(TeO_2)_{(100-x)} - (La_2O_3)_x$ glasses and **b** $(TeO_2)_{(100-x)} - (V_2O_5)_x$ glasses

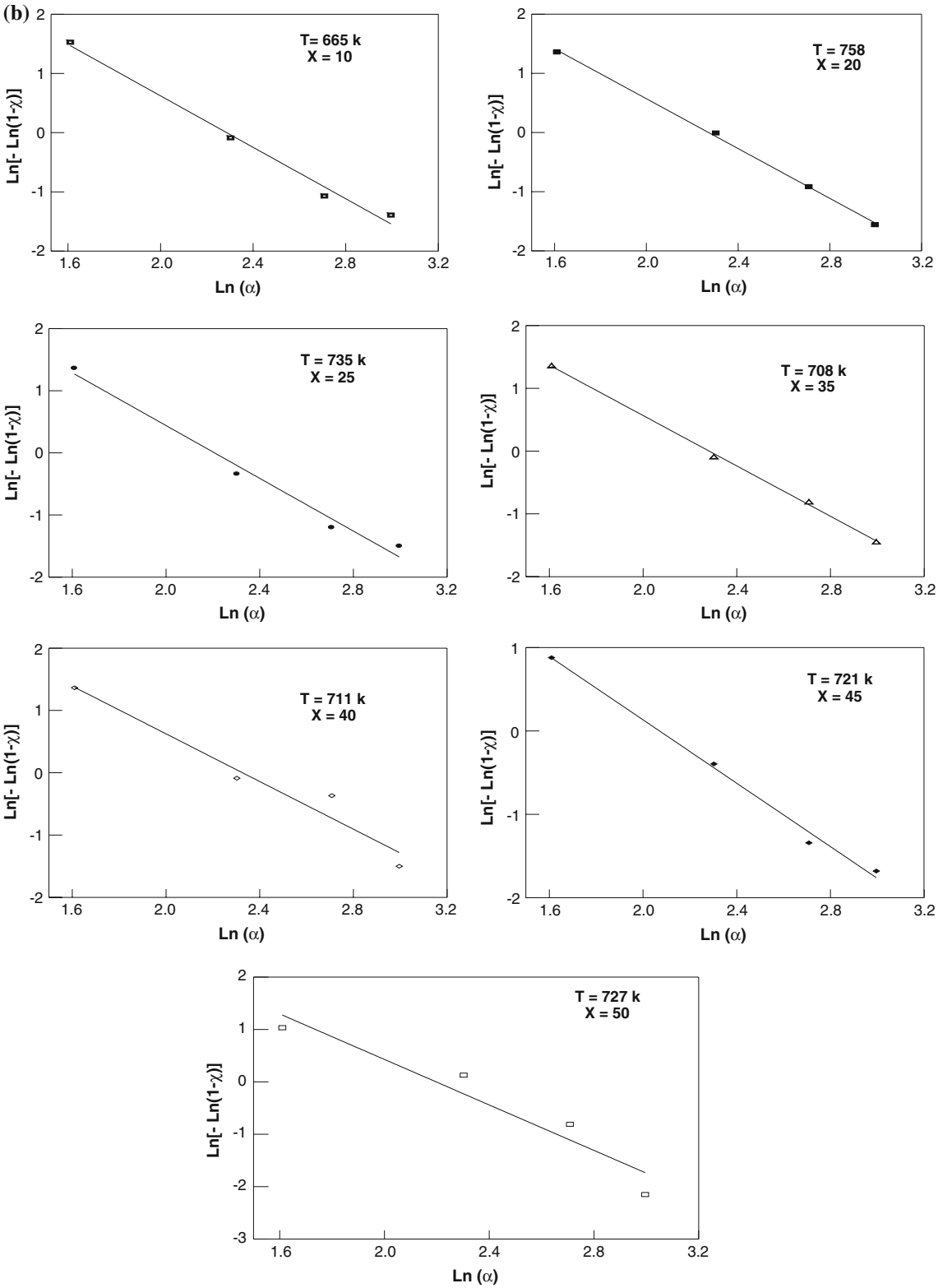

Fig. 11 continued

calculating this parameter, we conclude that the number of network bonds per unit volume, N_b, equals $7.74.10^{28}$ m^{-3} for pure TeO_2 glass. For binary TeO_2–La_2O_3 glass, the number of network bonds per unit volume increased from 8.07×10^{28} to 9.58×10^{28} m^{-3} with increasing La_2O_3 content from 5 to 20 mol%, and for TeO_2–V_2O_5, the

number of network bonds per unit volume decreased from 7.69×10^{28} to 6.36×10^{28} m^{-3} with increasing V_2O_5 content from 10 to 50 mol%. The average force constant of the glass $\bar{F}$ was given by the following relation:

$$\bar{F} = \frac{\{f_1(n_1)(N_c)_1 + f_2(n_2)(N_c)_2\}}{\{(n_1)(N_c)_1 + f(n_2)(N_c)_2\}} \quad (6)$$

where f is the stretching force constant of every cation–anion bond (calculated according to the empirical relation $f = 17/r^3$ from Ref. [16], where r is the ionic bond length), $(N_c)_1$ is the number of cations per glass formula unit $\sum_i (N_c)_i = xn_1 + (1-x)n_2$, for the multicomponent tellurite glasses in the form $xA_{n1}O_{m1} - (1-x)G_{n2}O_{m2}$ (where x is the mole fraction). Figure 5 shows a plot of average force constant versus mol% concentration of La_2O_3 and V_2O_5, respectively. The average force constant of TeO_2–La_2O_3 was decreased from 196.7 to 160.5 N/m with increasing La_2O_3 content from 5 to 20 mol%, and was increased from 234.8 to 264.8 N/m with increasing V_2O_5 content from 10 to 50 mol%. The quantitative analysis can be summarized as follows: for lanthanum tellurite glasses, the structure of the glass is weaker and more linked; the density data and molar volumes show that rare-earth oxides act as a network former rather than a network modifier in tellurite glass by increasing the crosslink density of TeO_2. For vanadium tellurite glasses, the density was decreased while the molar volume would be higher than pure TeO_2 glass, as shown in Table 1. From the change in the molar volume, it was clear that the corresponding structural units with its surrounding space increased by introducing vanadium oxides into the tellurite network, i.e., the basic structural units are linked more randomly.

Thermal results

The DSC curves for the glasses are shown in Fig. 6a, b for TeO_2–La_2O_3, and in Fig. 7a, b for TeO_2–V_2O_5. The curves show a very broad endothermic peak corresponding to the glass transition which is characterized by the temperature, T_g. As shown in Fig. 7a, this transition is followed by more than one exothermic peak corresponding to several crystallization temperatures, T_c. The two main successive crystallization peaks observed by increasing V_2O_5 mol%. This shows different stages of crystallization, in coincidence with previous study [17], and that some tellurite glasses are characterized by more than one crystallization mechanism. The first exothermic peak may be attributed to nucleation processes followed by the formation of a crystalline phase having a low internal free energy. The second peak at a higher temperature is attributed to the formation of a more relaxed crystalline phase. The approximate crystallization kinetics can be considered as follows. TeO_2 crystallizes in two main modifications [18]: orthorhombic β-TeO_2 tellurite and tetragonal α-TeO_2 paratellurite [19]. In both forms, the basic coordination polyhedron is a slightly distorted trigonal bipyramid with one equatorial position occupied by a one electron pair. The dependence of T_g on the type of modifier is given in Table 2. The increases in T_g induced by addition of the modifier could be explained by the increased degree of polymerization. T_x the temperature at which the crystallization process started was determined for the present glasses as shown in Table 2.

The values of the difference between T_g and T_x were calculated to illustrate the size of the working range between T_g and T_x. For pure TeO_2 glass, $T_x - T_g = 75$ K

Table 4 The order of the crystallization reaction at constant temperature, n, and the crystallization activation energy E_c (kJ/mol) in the binary tellurite glasses

Glass composition	n_1	n_2	E_c (kJ/mol) by the Coats–Redfern–Sestak model	E_c (kJ/mol) by Kissinger's model	E_c (kJ/mol) by Ozawa–Chen's model
TeO_2–La_2O_3					
92.5–7.5	1.3888		366.6	347.77	363.35
90–10	1.15		373.5	376.74	372.18
87.5–12.5	1.18		371.6	370.79	359.88
85–15	1.05		483.66	461.43	474.39
82.5–17.5	1.14		557.04	531.75	546.17
TeO_2–V_2O_5					
90–10	2.17		486.37	458.93	486.37
80–20	2.11		471.40	453.94	468.7
75–25	2.12		371.64	357.50	376.73
65–35	2.01		333.39	320.92	346.27
60–40	1.91		300.14	274.36	266.04
55–45	1.90	2.33	207.85	191.22	204.44
50–50	2.17	3.31	177.09	174.59	198.2

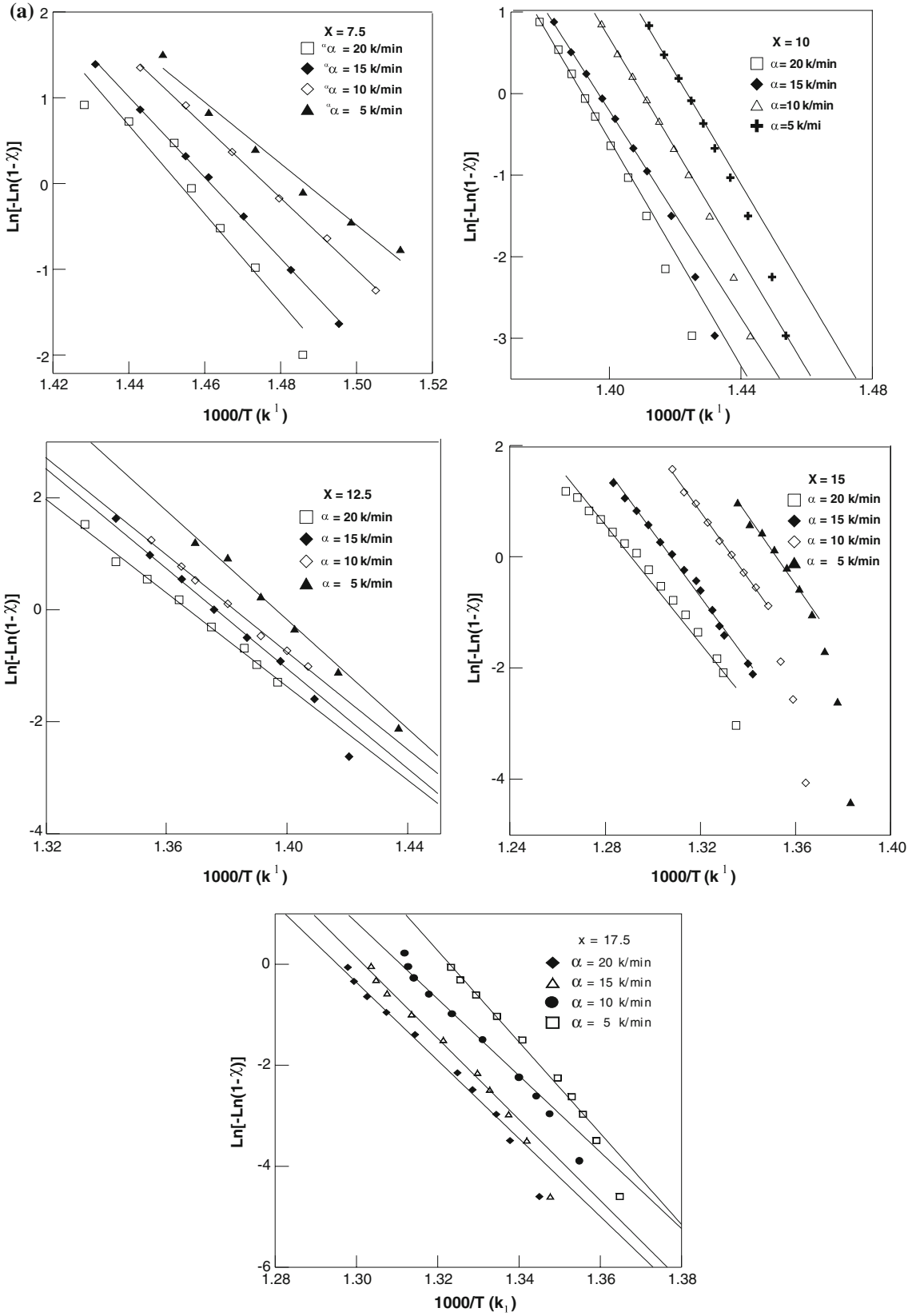

Fig. 12 The relation between $\ln(-\ln(1-\chi))$ versus $1000/T$ (K) at different heating rates for **a** $(TeO_2)_{(100-x)} - (La_2O_3)_x$ glasses and **b** $(TeO_2)_{(100-x)} - (V_2O_5)_x$ glasses

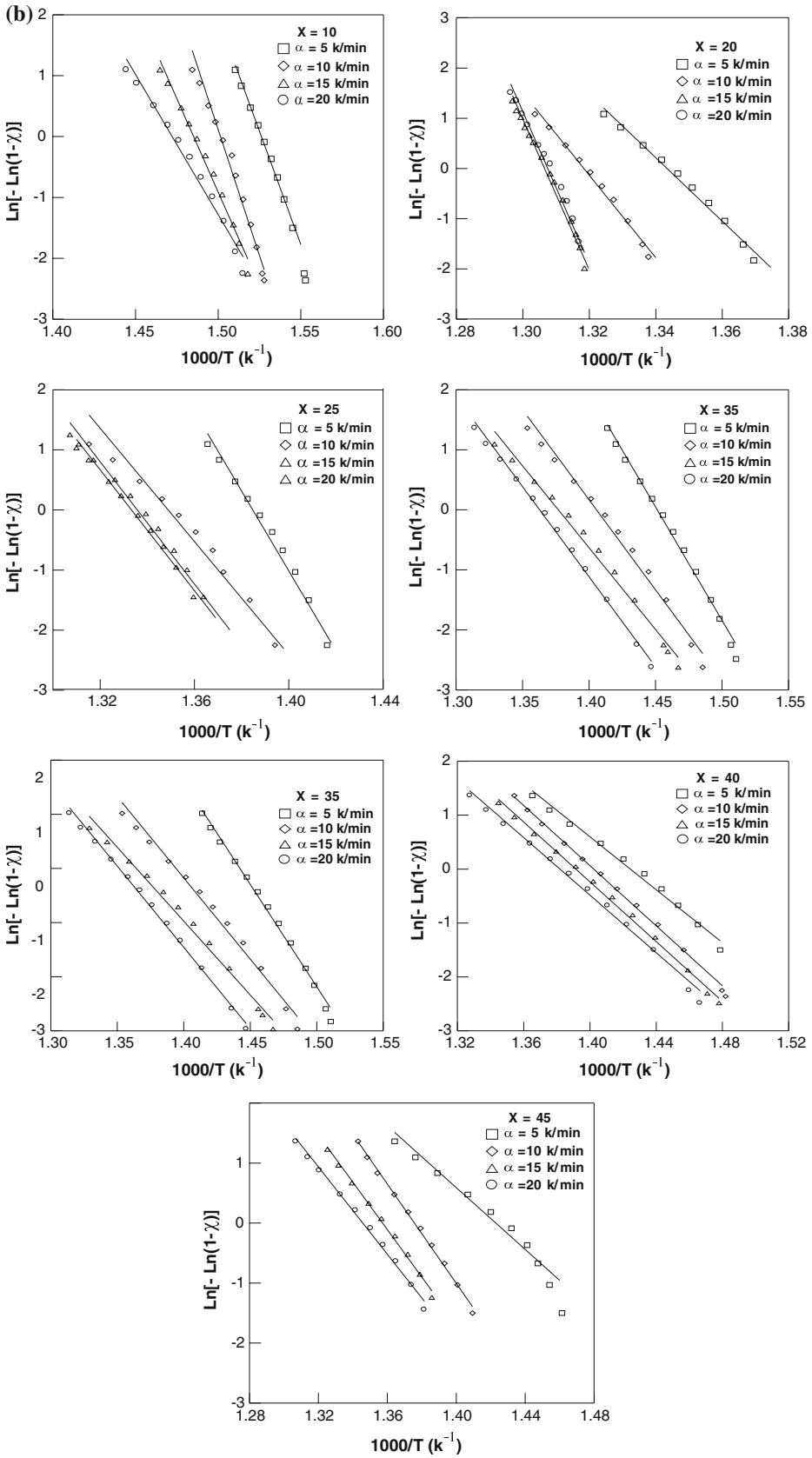

Fig. 12 continued

[4] and in this study changed from 37 to 22 K and from 83 to 175 K for binary tellurite-La_2O_3 and -V_2O_5, respectively. The values of T_m for all glasses obtained from the DTA curves were in the range 921–1180 K as shown in Table 2. The values of T_g/T_m were in the range 0.43–0.74. The glass-forming tendency, K_g, which was a useful parameter in comparing the devitrification tendency of the glass, is given by

$$K_g = \frac{T_c - T_g}{T_m - T_c} \tag{7}$$

and had the values of 0.47–0.21. As can be seen from Table 3, low values of K_g suggested high tendencies to devitrify. Previously, El-Mallawany [4] has calculated K_g for other binary tellurite vanadium tellurite glasses of the form TeO_2–MoO_3, TeO_2–Co_3O_4, and TeO_2–MnO_2 and found that the values of K_g were from 0.46 to 0.41, 0.33 to 0.31, and 0.45 to 0.4, respectively. The glass-forming tendency K_g of the present binary tellurite glasses decreases from 0.32 to 0.21 for lanthanum tellurite glasses system. The behavior is absolutely opposite in the second binary glass series become K_g increases from 0.31 to 0.47. Also the glass transition temperature, the activation energy of the glass transition E_t, and the crystallization activation energy E_c will be evaluated according to different models as stated in the following section.

Also, it is very important to analyze the variation of T_g in both tellurite glasses series as a function of both N_b and $\bar{F}$, i.e.,

$$T_g = f(N_b, \bar{F}) \tag{8}$$

From Tables 1 and 2, it is clear that for binary glass TeO_2–La_2O_3 the glass transition temperature T_g increased from 624 to 705 K, the number of network bonds per unit volume N_b increased from 8.069×10^{28} to 9.584×10^{28} m^{-3} and the average force constant $\bar{F}$ decreased from 196.7 to 160.5 N/m with increasing La_2O_3 content. While for TeO_2–V_2O_5, the glass transition temperature T_g decreased from 563 to 511 K, the number of network bonds per unit volume N_b decreased from 7.69×10^{28} to 6.36×10^{28} m^{-3} and the average force constant $\bar{F}$ increased from 234.8 to 264.8 N/m with increasing V_2O_5 content.

Glass transition temperature and glass transition activation energy

Firstly, the dependence of T_g on the heating rate α can be followed according to the empirical formula [20], as shown in Eq. 9.

$$T_g = A + B\ln(\alpha) \tag{9}$$

where A and B are constant for a given glass composition. The dependence of T_g on α is shown in Fig. 8a, b which indicates a relationship for the prepared glasses. The second and third approaches are the use of Kissinger's [20–23] and Moynihan's [24] formula, which is originally applied to crystallization studies as stated by Eqs. 10 and 11 where E_t is the glass transition activation energy. The dependencies of T_g on the heating rate α of the binary glasses were found to follow Eq. 10 and 11 which stated by Chen [22] and has often been used to calculate glass transition activation energy (E_t). Plots of $\ln(\alpha/T_g^2)$ versus $1/T_g$ for the prepared tellurite glasses indicate linearity as shown in Fig. 9a, b, the obtained values of E_t are shown in Table 3. E_t has also been calculated using the expressions as in Eqs. 10 and 11

$$\ln\left(\alpha \Big/ T_g^2\right) = \left(-E_t/RT_g\right) + \text{const.} \tag{10}$$

$$\ln(\alpha) = \left(-E_t/RT_g\right) + \text{const.} \tag{11}$$

Figure 10a, b shows the relation between $\ln(\alpha)$ and $1/T_g$ for the prepared glasses. The values of E_t deduced from this relation are obtained in Table 3. It is clear from the obtained data for the glass transition transformed temperature T_g at heating rate 10 K/min that the T_g depends upon:

- Tellurite glasses with higher percentage of La_2O_3 have the higher values of T_g, and with higher percentage of V_2O_5 has the lower values of T_g, i.e., La_2O_3 creates a more strengthen tellurite glass.
- The glass transition activation energy E_t of La_2O_3 tellurite glass has been increased from 296 to 403.9 kJ/mol by increasing La_2O_3 from 7.5 to 17.5 mol% (by using Moynihan's model) while it has been increased from 285.71 to 392.32 kJ/mol for the same amount of La_2O_3 (by using Chen's model), so both models confirm each other.

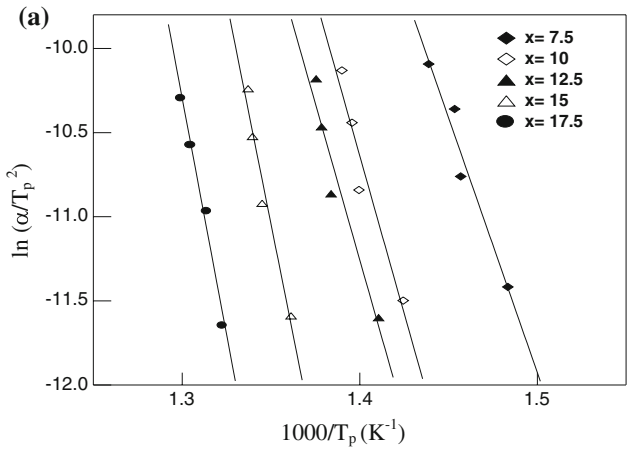

Fig. 13 Variation of $\ln(\alpha/T_p^2)$ versus $(1000/T_p)$ for **a** $(TeO_2)_{(100-x)} - (La_2O_3)_x$ glasses and **b** $(TeO_2)_{(100-x)} - (V_2O_5)_x$ glasses

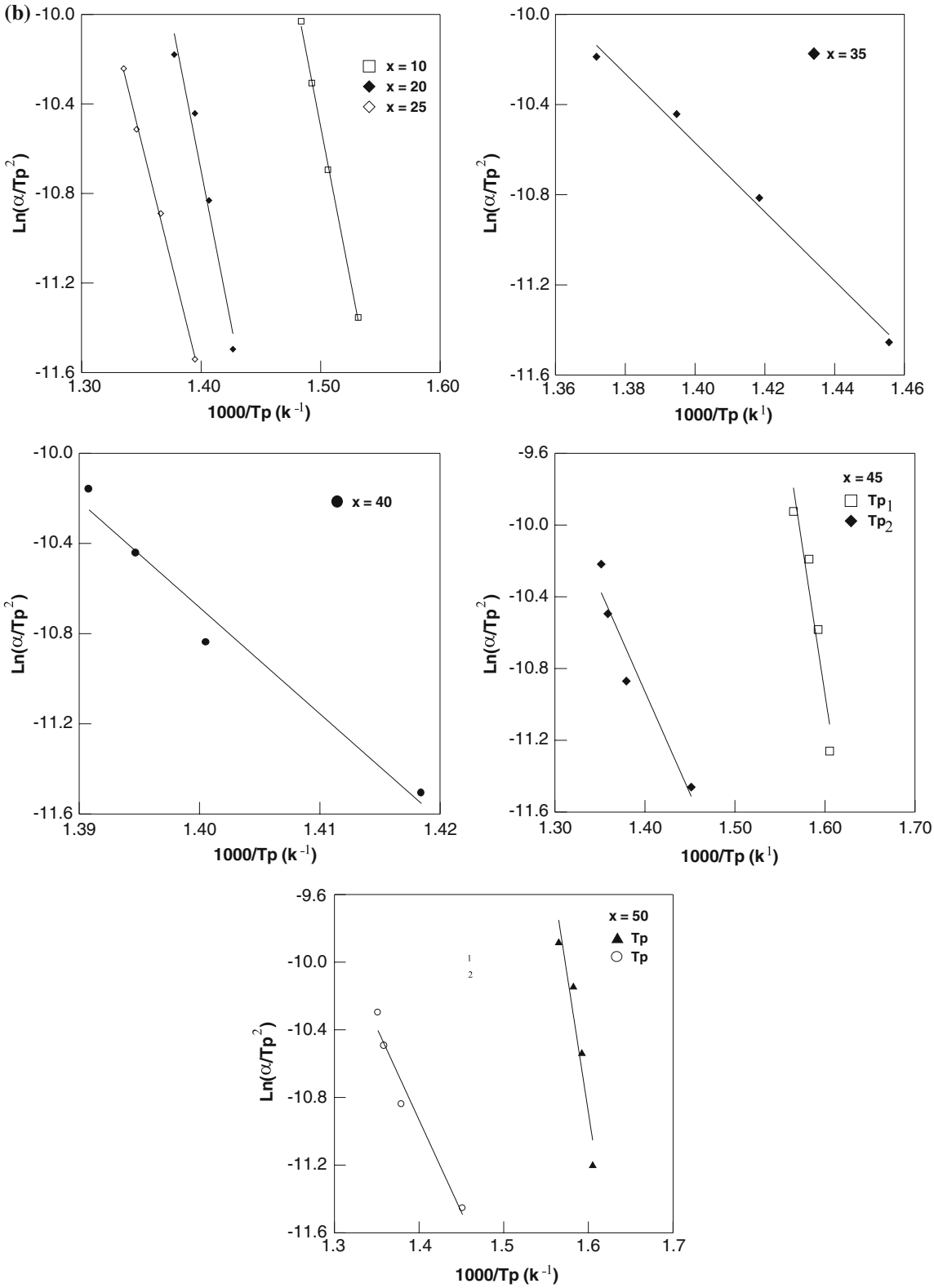

Fig. 13 continued

Also the glass transition activation energy E_t of V_2O_5 tellurite glasses has been decreased from 594.96 to 289.79 kJ/mol by increasing V_2O_5 from 10 to 50 mol% (by using Moynihan's model), while it has been decreased from 585.58 to 281.25 kJ/mol for the same amount of V_2O_5 (by using Chen's model), so both models confirm each other.

Crystallization temperature and crystallization activation energy

Kissinger [21] developed a method which is commonly used in analyzing crystallization data in DSC and DTA experiments. While the method proposed by Ozawa [25] is used to deduce the order of the crystallization reaction (n) at constant temperature

$$d\{\ln[-\ln(1-\chi)]\}/d\{\ln(\alpha)\} = -n \quad (12)$$

where α is heating rate of binary glass and χ is the volume fraction crystallized in time t.

On this basis, plotting $\ln[-\ln(1-\chi)]$ versus $\ln(\alpha)$, which is obtained at the same temperature from a number of crystallization exotherms taken at different heating rates, should yield the value of the order of the crystallization reaction (n) at constant temperature n. Now to deduce the order of crystallization, the value of (n) is evaluated by plotting $\ln[-\ln(1-\chi)]$ versus $\ln(\alpha)$, where χ is obtained from the crystallization exothermic peaks at the same temperature taken at deferent heating rates. Figure 11a, b shows the plots of $\ln[-\ln(1-\chi)]$ versus $\ln(\alpha)$ at different constant values of temperature. From the slopes of this relation, the value of n is equal to 1.38, 1.15, 1.18, 1.05, and 1.14, respectively, by increasing La_2O_3 from 7.5 to 17.5 mol%, whereas n is equal to 2.17, 2.11, 2.12, 2.01, 1.91, 1.90, and 2.17, respectively, at the first crystallization peaks by increasing V_2O_5 from 10 to 50 mol% and at the second crystallization peaks n is equal to 2.33 and 3.31 for 45 and 50 mol% of V_2O_5 as tabulated in Table 4. The values of the crystallization activation energy (E_c) calculated by using the methods of Coast–Redfern–Sestak [26], Kissinger [27], and modified Ozawa and Chen [22, 25]. The values of crystallization activation energy E_c calculated for all the heating rates by using method of Coast–Redfern–Sestak [26]. Figure 12a, b shows the plots of $\ln[-\ln(1-\chi)]$ versus $1/T$ at different heating rates, from the slopes the average values of the crystallization activation energy of the prepared glasses for the first crystallization peak are calculated and obtained in Table 4. The values of the crystallization activation energy (E_c) calculated using Kissinger's method and modified Ozawa–Chen equation from Figs. 13a, b and 14a, b are obtained in Table 4. It has been found that the crystallization activation energy E_c by using Kissinger's method increased from 347.77 to 531.75 kJ/mol due to increasing of La_2O_3 in the glasses from 7.5 to 17.5 mol% and also the same behavior by Ozawa–Chen model and Coast–Redfern–Sestak are found. But due to increasing of V_2O_5 in the glasses from 10 to 50 mol% the first crystallization activation energy E_{c1} decreased from 458.93 to 174.59 kJ/mol. The second crystallization activation energy E_{c2} is equal to 318 and 332 kJ/mol at 45 and 50 V_2O_5 mol% and also the same behavior by Ozawa–Chen model and Coast–Redfern–Sestak are found. According to the cluster model of glasses [28], the vitreous state $(TeO_2)_{100-x} - (V_2O_5)_x$ may in some way consist of a mixture of extremely small crystallites of size less than 10 nm of the two polymorphic phases of TeO_2, which forms the essential framework of the glass matrix together with small regions proportional to the concentration of the added modifier. As the temperature is raised to the point at which significant solid-state diffusion of atoms or groups of atoms can occur, that is above T_g, the diffusion of clusters of size <3 nm, together with statistical collisions between them, results in these clusters coalescing. Clusters which differ very little in free energy and orientation collide in such a way that interfaces with minimum strain are established between them. Such an assemblage of clusters results in partial crystallization, as the α-TeO_2 phase is formed. Above the first crystallization peak, there is still some persisting amorphous phase, representing the remaining clusters of the other polymorphic phase of TeO_2 with more highly strained interfaces. On a further increase in temperature, these highly strained interfaces have the opportunity to relax. Such relaxation occurs by acquiring atoms with the appropriate orientation and releasing the strain in the interfaces the neighboring clusters and to the liquid phase. In this way, through statistical collisions clusters of the remaining polymorphic phase could assemble with minimum or zero strained interfaces and crystallize to form β-TeO_2. This second stage of crystallization is observed as the second weak exothermic peak, in the glasses containing Vanadium oxide. The above experimental results will complete the previous research on binary tellurite glasses either in the thermal, structural, vibrational, elastic, electrical, or optical research directions [2–9, 29–40].

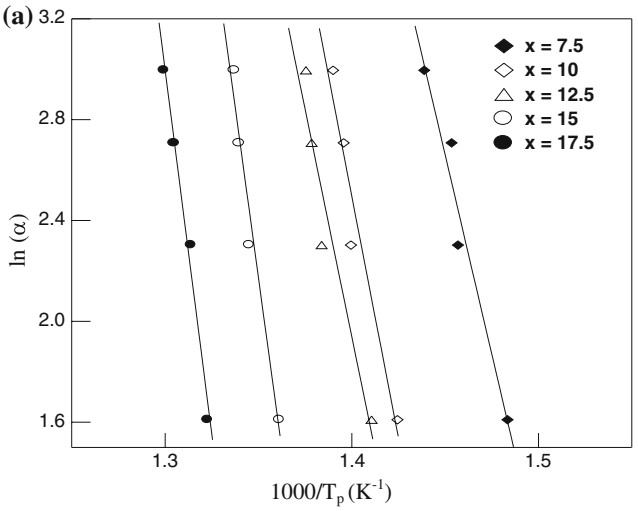

Fig. 14 Variation of $\ln(\alpha)$ versus $(1000/T_p)$ for **a** $(TeO_2)_{(100-x)} - (La_2O_3)_x$ glasses and **b** $(TeO_2)_{(100-x)} - (V_2O_5)_x$ glasses

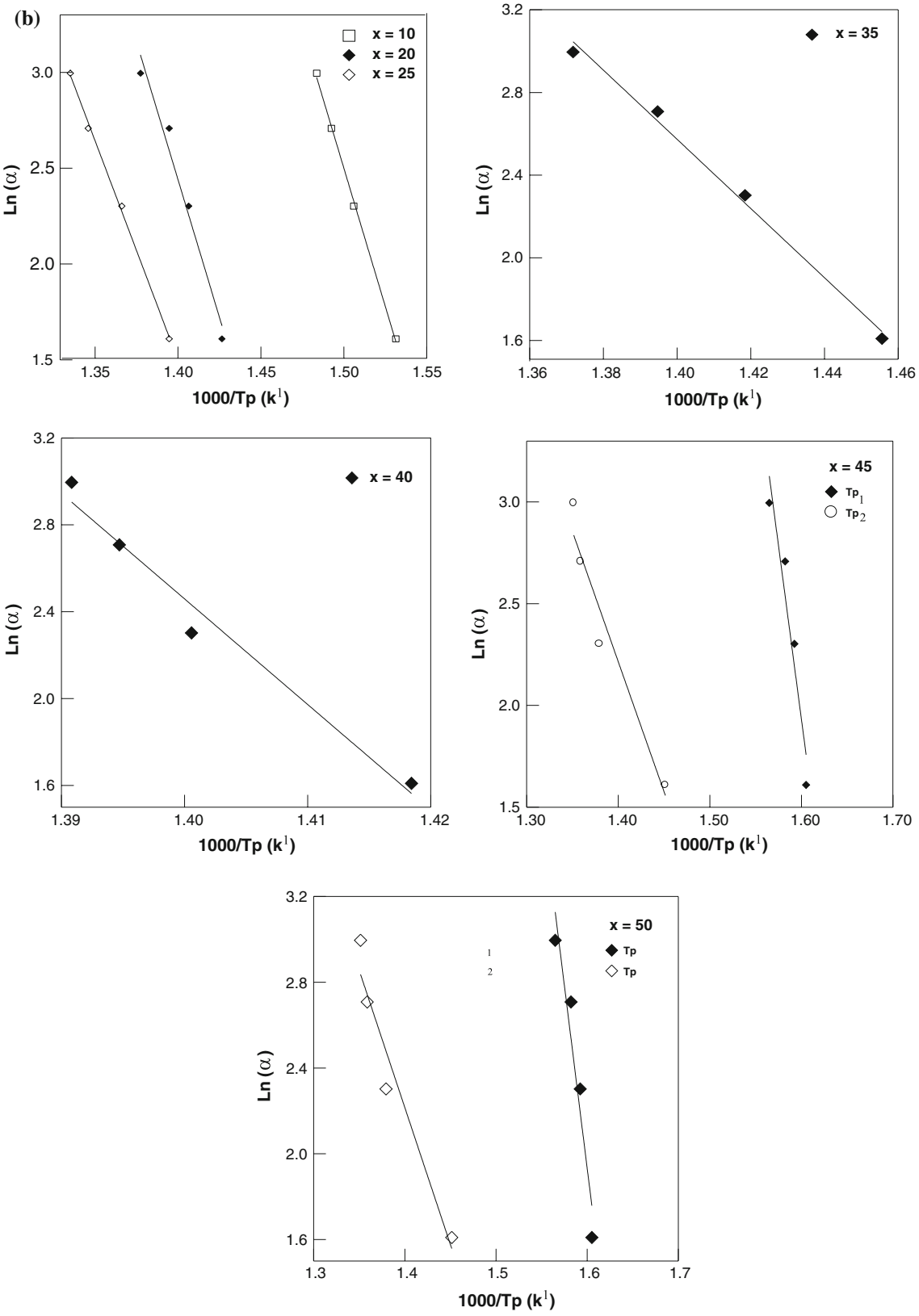

Fig. 14 continued

Conclusion

Binary tellurite glasses in the form $TeO_2(100 - x) - xA_nO_m$ where $A_nO_m = La_2O_3$ or V_2O_5 and $x = 5$, 7.5, 10, 12.5, 15, 17.5, and 20 mol% for La_2O_3 and 10, 20, 25, 30, 35, 40, 45, and 50 mol% for V_2O_5 were prepared and investigated for the thermal properties. The thermal properties, such as glass transition temperature T_g, crystallization temperature T_c, the onset of crystallization temperature T_x, glass stability against crystallization S and glass-forming tendency K_g, specific heat capacity C_p, were measured and quantitatively analyzed according to the number of bonds per unit volume, the crosslinked density, and the average stretching force constant. The glass transformation energy has been calculated using Chen's and Moynihan's formulas, both models are very close for every glass series. The crystallization energies of these glasses have been calculated using Kissinger's, Ozawa–Chen's, and Coast–Redfern–Sestak's models.

References

1. El-Mallawany R (2002) Tellurite glass handbook: physical properties and data. CRC Press, FL, USA (International Materials Institute for New Functionality in Glass (IMI-NFG), Lehigh University, USA (2005) www.lehigh.edu/imi/resources.htm)
2. El-Mallawany R, Aboushely A, Rahamni A, Yousef E (1997) Phys Status Solidi A 163:377
3. El-Mallawany R (1992) J Mater Res 7:224
4. El-Mallawany R (1995) J Mater Sci Electron 6:1
5. El-Mallawany R, Hagar I, Poulain M (2002) J Mater Sci 37:3291. doi:10.1023/A:1016195303433
6. El-Mallawany R (2000) Phys Status Solidi A 177:439
7. El-Mallawany R (2000) Mater Chem Phys 63:109
8. El-Mallawany R (2003) J Mater Res 18(2):402
9. El Mallawany R, Abbas Ahmed I (2008) J Mater Sci 43:5131. doi:10.1007/s10853-008-2737-4s
10. Moawad H, Jain H, El-Mallawany R, Ramadan T, ElSherbine M (2002) J Am Ceram Soc 85:11
11. Moawad H, Jain H, El-Mallawany R (2009) J Phys Chem Solids 70:224
12. Kim S, Yako T, Sakka S (1993) J Am Ceram Soc 76:2486
13. Lambson EF, Saunders GA, Bridge B, El-Mallawany RA (1984) J Non-Cryst Solids 69:117
14. Havinga E (1961) J Phys Chem Solids 18:253
15. Mukherjee S, Ghosh U, Basu C (1992) J Mater Sci Lett 11:985
16. Bridge B, Higazy AA (1986) J Phys Chem Glasses 27:1
17. Kozhukharov VS, Nikolov S, Marinov M (1979) J Mater Res Bull 14:735
18. Beyer H (1967) Z Kristallogr 124:228
19. Johnson PAV, Wright AC, Yarker CA, Sincair RN (1986) J Non-Cryst Solids 81:163
20. Lasocka M (1979) Mater Sci Eng 23:173
21. Kissinger HE (1956) J Res NBS 57:217
22. Chen H (1978) J Non-Cryst Solids 27:257
23. Shelby J (1979) J Non-Cryst Solids 34:111
24. Moynihan CT, Easteal AJ, Wider J, Tucker J (1974) J Phys Chem 78:2673
25. Ozawa T (1965) Bull Chem Soc Jap 38:351
26. Coats W, Redfern JP (1964) Nature 201:86
27. Kissinger HE (1957) Anal Chem 29:1702
28. Goodman CHN (1987) J Glass Technol 28:19 (1987)
29. El-Mallawany R, El-Khokany N, Afifi H (2006) Mater Chem Phys 95:321
30. Sidky M, El-Mallawany R, Abousehly A, Saddeek Y (2002) Mater Chem Phys 74:222
31. Sidky M, El-Mallawany R, Abousehly A, Saddeek Y (2002) Glass Sci Technol 75:87
32. Abdel Kader A, El-Mallawany R, ElKholy M (1993) J Appl Phys 73:75
33. Hampton R, Hong W, Saunders G, El-Mallawany R (1987) J Non-Cryst Solids 94:307
34. Hampton R, Hong W, Saunders G, El-Mallawany R (1988) Phys Chem Glasses 29:100
35. ElKholy M, El-Mallawany R (1995) Mater Chem Phys 40:163
36. El-Mallawany R, El-Deen LS, Elkholy M (1996) J Mater Sci 31:6339. doi:10.1007/BF00354458
37. El-Mallawany R, El-Said Adly, El-Gawad M (1995) Mater Chem Phys 41:87
38. Abdel Kader A, El-Mallawany R, ElKholy M (1994) Mater Chem Phys 36:365
39. Sooraj Hussain N, Hungerford G, El-Mallawany R, Gomes MJM, Lopes MA, Ali N, Santos JD, Buddhudu S (2008) J Nanosci Nanotechnol 8:1
40. El-Mallawany R, Dirar Abdalla M, Abbas Ahmed I (2008) Mater Chem Phys 109:291